







Article

A Spectral–Spatial Approach for the Classification of Tree Cover Density in Mediterranean Biomes Using Sentinel-2 Imagery

Michail Sismanis * , Ioannis Z. Gitas , Nikos Georgopoulos , Dimitris Stavrakoudis , Eleni Gkounti 
and Konstantinos Antoniadis 

Laboratory of Forest Management and Remote Sensing, School of Forestry and Natural Environment, Aristotle University of Thessaloniki, P.O. Box 248, 54124 Thessaloniki, Greece; igitas@for.auth.gr (I.Z.G.); georgopn@for.auth.gr (N.G.); jstavrak@for.auth.gr (D.S.); gkountie@for.auth.gr (E.G.); konstanag@for.auth.gr (K.A.)

* Correspondence: msismanis@for.auth.gr

Abstract: Tree canopy cover is an important forest inventory parameter and a critical component for the in-depth mapping of forest fuels. This research examines the potential of employing single-date Sentinel-2 multispectral imagery, combined with contextual spatial information, to classify areas based on their tree cover density using Random Forest classifiers. Three spatial information extraction methods are investigated for their capacity to acutely detect canopy cover: two based on Gray-Level Co-Occurrence Matrix (GLCM) features and one based on segment statistics. The research was carried out in three different biomes in Greece, in a total study area of 23,644 km². Three tree cover classes were considered, namely, non-forest (cover < 15%), open forest (cover = 15%–70%), and closed forest (cover ≥ 70%), based on the requirements set for fuel mapping in Europe. Results indicate that the best approach identified delivers F1-scores ranging 70%–75% for all study areas, significantly improving results over the other alternatives. Overall, the synergistic use of spectral and spatial features derived from Sentinel-2 images highlights a promising approach for the generation of tree cover density information layers in Mediterranean regions, enabling the creation of additional information in support of the detailed mapping of forest fuels.



Citation: Sismanis, M.; Gitas, I.Z.; Georgopoulos, N.; Stavrakoudis, D.; Gkounti, E.; Antoniadis, K. A Spectral–Spatial Approach for the Classification of Tree Cover Density in Mediterranean Biomes Using Sentinel-2 Imagery. *Forests* **2024**, *15*, 2025. <https://doi.org/10.3390/f15112025>

Academic Editor: Xiangdong Lei

Received: 27 September 2024

Revised: 2 November 2024

Accepted: 15 November 2024

Published: 18 November 2024



Copyright: © 2024 by the authors. Licensee MDPI, Basel, Switzerland. This article is an open access article distributed under the terms and conditions of the Creative Commons Attribution (CC BY) license (<https://creativecommons.org/licenses/by/4.0/>).

Keywords: Sentinel-2; spectral–spatial approach; tree cover density

1. Introduction

Forests are complex ecosystems that play a critical role in the Earth’s biosphere and affect many natural processes [1]. They facilitate water and energy exchanges, provide habitat for diverse flora and fauna, regulate global climate, and provide vital ecosystem services [2]. The management of forests requires accurate and up-to-date information in terms of forest structure and its dynamic changes [3]. One of the most common parameters that is used as an indicator of the structural and functional properties of forests is tree canopy cover, which is usually defined as the percentage of land area covered by the vertical projection of tree crowns on the horizontal plane [4]. Canopy cover can be used in multiple different scientific fields, e.g., hydrometeorology [5], assessment of soil erosion [6], wildlife habitat characterization [7], and monitoring of regeneration dynamics [8], to name a few.

Measuring tree cover was traditionally performed by field sampling, which is an arduous and costly process requiring many sampling points for accurate estimations [9], especially in large areas. Most of these plot-based studies on forest cover are able to provide accurate stand level information, but on a broader scale, they might encounter inaccuracies [10]. With the increasing utilization of remote sensing technologies, there is a growing international trend for the development of approaches that could potentially estimate canopy cover through satellite sensors, allowing for cost-efficient solutions [11,12]. The use of such sensors would enable the capacity to detect and map dynamic changes in

land cover and structural forest characteristics in a systematic and updatable manner, in increased spatial and temporal scales [13,14].

Multispectral satellite sensors can indirectly measure the percentage of canopy cover by making a direct connection with leaf area, a component that can be detected and effectively differentiated from other landscape components, i.e., bare ground, based on the remote sensing properties of each one. The estimation of tree canopy cover from optical satellite data is a research topic that has been extensively addressed by researchers in recent literature. A variety of different sensors has been investigated in terms of their capacity to monitor canopy cover, such as Landsat TM [15–18], Landsat-8 OLI [19], MODIS [20], AVNIR-2 [21], and Sentinel-2 [22–25]. Especially, the new generation of medium resolution (10 to 30 m) satellite sensors, i.e., Sentinel-2 and Landsat-8, have become popular for similar tasks based on their spatiotemporal coverage and free availability, with Sentinel-2 reported to provide the best performance of the two [23,26,27]. Additionally, the combination of multispectral data with other data sources, i.e., Airborne Light Detection and Ranging (LiDAR), can further enhance the classification performance and can consistently outperform passive sensors alone [16,28–31]. However, the high acquisition costs and the small spatial coverage of these methods tend to limit results to smaller regional scales.

Researchers have used various parametric and non-parametric models for predicting canopy cover, with the latter being identified as the better option [27]. One non-parametric machine learning approach that is considered one of the most widely used is the random forest (RF) algorithm [32]. RF algorithms offer stability and robustness, are easy to train, resistant to overfitting, and offer very good performance [33–38]. Several recent studies have highlighted RF as one of the best approaches for ecological modeling tasks, e.g., biomass estimation [39] and land cover classification [40]. Especially in terms of tree canopy cover, RF is one of the most frequently used approaches with numerous recent studies highlighting its performance and efficiency [24,27,41–45].

A growing trend among recent research is the orientation toward more contextual classification algorithms, i.e., algorithms that are able to combine information from multiple sources. More specifically, spectral–spatial approaches are one such line of research, aiming to extract meaningful data by also analyzing the underlying spatial patterns between pixels. Some of the most recent studies that address the topic of tree cover density make use of the Gray-Level Co-Occurrence matrix (GLCM) [46] in very high [47,48] and medium resolution [48,49] images, Convolutional Neural Networks (CNNs) [50], and multispectral unmixing with contextual spatial information [51].

In terms of large-scale mapping, several different works have tried to address the mapping of tree cover and its changes on a global [11,12,52,53] or on a continental scale [54–57], with very promising results. Currently, some of the most widely used tree coverage products are the global MODIS VCF and the global tree cover product at 30 m generated by Sexton et al. [12,48,58]. These published products have medium-to-coarse spatial resolutions, making them suitable for analyzing changes in tree cover over large areas, while at the same time maintaining good levels of detail [52,59]. In all the aforementioned works, multispectral images form the core input data sources on account of their spatio-temporal coverage, free availability, and their capacity to upscale results, which can be further augmented with thematic maps or 3D data to achieve even greater accuracies [60–62].

Large-scale tree cover products are a valuable and cost-efficient source of information, allowing quick integration into other services and facilitating the generation of added-value products [63], especially when there are no other alternatives available in finer spatial scales. However, some of the reported drawbacks are that they have a tendency to underestimate tree cover [8] and produce unreliable results in small areas with mixed vegetation [64]. In the recent past, a notable increase in the frequency and intensity of wildfire events has been observed, especially in Mediterranean countries [65]. Based on the most recent advances in terms of wildland fuel mapping in Europe [63], tree canopy cover is an essential component in the complete characterizations of fuels, and thus its accurate estimation is critical in wildfire prevention and risk assessment actions, e.g., reduction in fuel load in areas with

high risk. The capacity to generate updatable and accurate tree cover density information over large areas would significantly benefit wildfire management across large and diverse landscapes. Furthermore, it will provide an alternative to the use of static (and potentially outdated) products, which is one of the main sources of tree cover data that are used in fuel mapping processes in Greece [66,67]. Static products, while easy to use and integrate into processing chains, have a temporal lag and may not capture dynamic changes in forest cover, potentially misleading fire danger assessments in fire-prone regions with rapid vegetation interchanges.

Challenges still remain in the estimation of tree cover density from remote sensing sensors, such as the saturation effect in the identification of high-density vegetation traits [68]. However, in an operational context when the timely delivery and updateability of the products are important, satellites like Sentinel-2 can be a valuable tool, with recent research highlighting the need for the development of more accurate methods for tree cover estimation [69].

The present study examines the generation of tree cover density maps in Mediterranean ecosystems using a spectral–spatial approach that requires a single Sentinel-2 image from the summer season. Three broad tree cover density classes are considered, following the guidelines set by recent advances in fuel mapping in European territories [63]. Three different spatial information extraction techniques are investigated and assessed for their capacity to enhance the accuracy of the final products, with the fusion of spectral and contextual spatial data being performed by Random Forest (RF) classifiers. Through the methodology presented in this research, accurate and updatable tree cover density maps can be generated for Mediterranean biomes, providing a valid alternative that enables the use of up-to-date information in support of wildland fuel mapping initiatives.

2. Materials and Methods

2.1. Study Area

The present research was carried out in three different biomes in Greece (Table 1) (Figure 1). Each region is comprised of at least two NUTS3 regional units, with a total study area of approximately 23,644 km². Each biome was selected based on its vegetation and landscape characteristics, encompassing different vegetation dynamics in Mediterranean ecosystems, and can be considered representative of conditions typically encountered

Table 1. Administrative regions and total area extend for each study area selected.

Study Area	NUTS3 Regions	Total Area (km ²)
A	Achaia, Ilia, and Etoloakarnania	11,312
B	Ioannina and Arta	6599
C	Pella, Imathia, and Pieria	5732

Biome A is located in southwestern Greece and is comprised of the regional units of Achaia, Ilia, and Etoloakarnania. It covers an area of approximately 11,312 km², with elevation ranging from 0 to 2504 m. It is a typical Mediterranean landscape with high variation in topography. Low-altitude areas contain common Mediterranean vegetation species (i.e., *Olea europaea* L., *Ceratonia siliqua* L., *Quercus ilex* L., *Quercus frainetto* Ten., *Quercus coccifera* L., *Quercus pubescens* Willd., *Pistacia lentiscus* L., *Phillyrea latifolia* L., *Pinus halepensis* Mill., *Pinus Brutia* Ten.), while sub-alpine species can be encountered in the higher altitudes (i.e., *Fagus* sp., *Pinus sylvestris* L., and *Pinus nigra* J.F. Arnold, *Abies Cephalonica* Loudon, *Juniperus nana* Willd., and *Juniperus foeditissima* Willd). Shrublands are the dominant type of land cover in this region, covering the largest part of the vegetated areas, with needleleaf forests being located in specific regions.

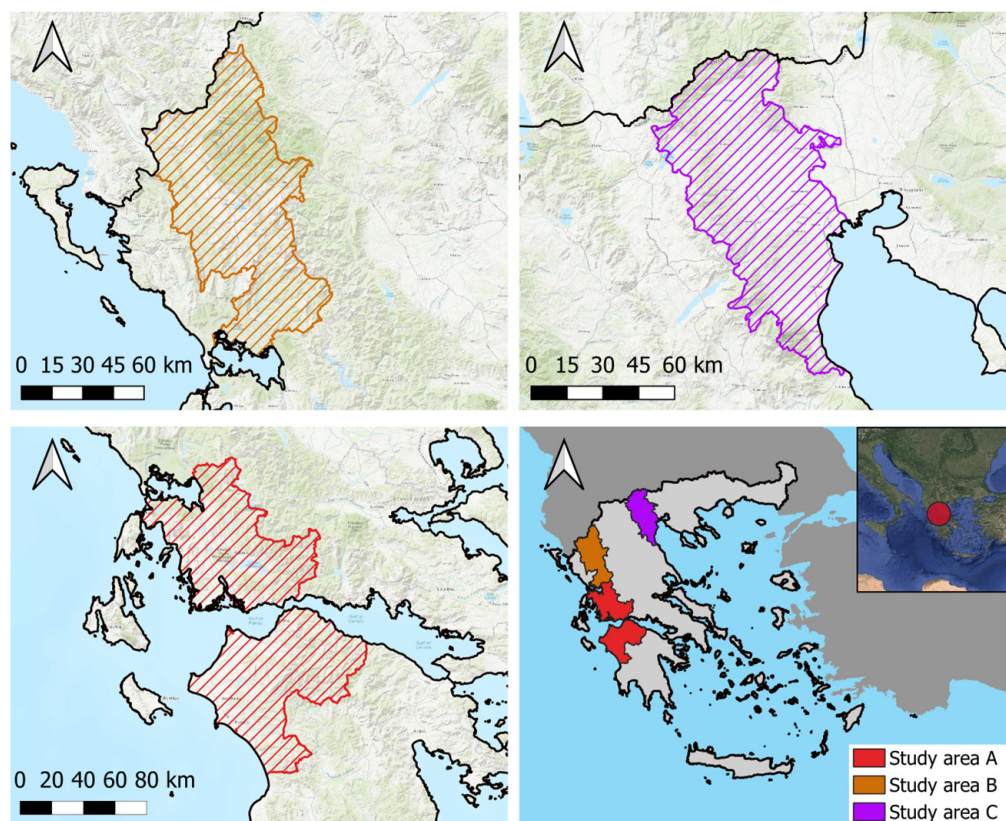


Figure 1. Map of the three different biomes examined in this study in Greece.

Biome B is located in mainland Greece and is comprised of the regional units of Ioannina and Arta, covering an area of 6599 km². Its elevation varies from 0 to 2624 m above sea level. The landscape exhibits a complex vegetation structure comprised mainly of evergreen broadleaves, conifers, and shrubs covering the main bulk of the area. Some of the most widespread species in this region are *Fagus sylvatica* L., *Betula pendula* Roth, *Pinus sylvestris* L., *Carpinus betulus* L., *Quercus petraea* (Matt.) Liebl, *Acer pseudoplatanus* L., and *Acer platanoides* L.. In this biome, forests are more widespread, with a bigger abundance of forest species when compared with biome A.

Finally, biome C is located in the northern part of Greece and is comprised of the regional units of Pella, Imathia, and Pieria. It covers an area of approximately 5732 km². Biome C contains the highest mountain in Greece, i.e., Mount Olympus, with the elevation of the study area ranging from 0 to 2917 m above sea level. The vegetation is characterized by a very high diversity, with the study area mainly covered by dense forests, comprised of broadleaved deciduous species such as *Fagus* and *Quercus* pure stands, or sometimes mixed with other deciduous species.

2.2. Input Data

The mapping approaches presented make use of optical data from a single Sentinel-2A L2A Multispectral Instrument (MSI) image acquisition. The images were selected in the summer months, preferably mid-July to mid-August (Table 2), on days when cloud cover was minimal. Seven spectral bands were used, more specifically, B02 (Blue), B03 (Green), B04 (Red), B06 (Red-edge), B8A (Narrow NIR), B11 (SWIR1), and B12 (SWIR2). The spatial resolution of all bands was 20 m. Images were downloaded as MSI-L2A products, which are atmospherically corrected images that do not require any further corrections. Processing was only carried out in regions that were labeled as vegetated, i.e., areas that were labeled as agricultural or urban were excluded from any further processing. To correctly delineate the boundaries of the different types of land use, auxiliary geographic data from the base

maps of the national forest inventory of 2022 were used. Furthermore, recent burned areas from the fire seasons of 2018 to 2022 were also masked out of the process using burned area maps that were provided by the NOFFi Operational Burned Area Mapping Service (NOFFi-OBAM) [70]. All sampling points located inside the burned area perimeters were discarded to make sure that no erroneous data were inserted into the training or validation processes. Additionally, all damaged areas were considered non-forest for the rest of the research, as the scope of the work encompasses the mapping of tree cover density in regions that have not been impacted by wildfires.

Table 2. Sentinel-2 images used for the supervised classification of tree cover density.

Study Area	Acquisition Data	Type
A	16 August 2022	Sentinel-2A MSI L2A
B	15 July 2022	Sentinel-2A MSI L2A
C	22 July 2022	Sentinel-2A MSI L2A

2.3. Training Patterns

In the context of this work, a separation in three broad tree cover density classes was examined: (A) non-forest, (B) open forest, and (C) closed forest (Table 3). The classification scheme followed in this paper was established by Aragoneses et al. [63], who defined that in the context of fuels, a more general separation of tree cover density is preferable. It should also be mentioned that, for the purposes of this research, the classification does not take into account species or vegetation type information, only the presence/absence of forest species and whether their cover density can be inferred using a single Sentinel-2 image. As a result, the first class, i.e., non-forest, is a broader class that encompasses different types of land cover, such as shrublands, grasslands, and non-vegetated areas. On the other hand, open forest and closed forest classes refer to any combination of needleleaved or broadleaved forest species that fall within the respective class density limits. Furthermore, understory structure and composition are not addressed in this work.

Table 3. Classification scheme and types of vegetation considered for the identification of tree cover density.

Class Name	Tree Cover Density	Types of Vegetation Cover
Non-forest	<15%	Shrublands, grasslands, and non-vegetated areas
Open forest	≥15% and <70%	Broadleaved and needleleaved forest species
Closed forest	≥70%	Broadleaved and needleleaved forest species

To extract the training data to be used in supervised classification algorithms, a series of training patterns were generated for all classes of interest using stratified random sampling based on fuel type maps provided by NOFFi [70]. Each of the sampling points was photo-interpreted using Google Earth and any required corrections were made to ensure the final correct assignment in the proper classes. In the case that a significant change took place, e.g., wildfire, the points were discarded from the training set. In total, 7282 training points were used. The distribution of the sampling points across the different classes and study areas can be found in Table 4.

Table 4. Training points generated for the extraction of the dataset per study area.

Classes	Training Points	Study Area
Non-forest	599	A
Open forest	364	
Closed forest	267	
Total	1230	
Non-forest	1597	B
Open forest	916	
Closed forest	998	
Total	3511	
Non-forest	631	C
Open forest	258	
Closed forest	1652	
Total	2541	

2.4. Classification Methodology

Four approaches were examined for the mapping of the tree cover density classes. The first relies on a single Sentinel-2 image, used as a reference method. The other three methods investigated perform an extraction of contextual spatial information from the spectral data, and combine both to enhance classification accuracy. One of the most common methods for the extraction of spatial information from multi-band raster datasets is the implementation of a Principal Component Analysis (PCA). Instead of applying spatial information extraction techniques in all bands, it is possible to use only the first Principal Component (PC1), without significantly affecting the results [71]. The first approach for the extraction of contextual spatial information is based on the Grey Level Co-occurrence Matrix (GLCM) [46], an established and widely used approach for textural information extraction. There are many textural features that can be calculated using the GLCM approach. However, certain GLCM features are correlated, and it is advised in most cases to include only a certain number of them to reduce the complexity [71]. In the context of this research, 4 GLCM textural features are considered, namely, entropy, correlation, contrast, and inverse difference moment (IDF) (Table 5). The computation of GLCM information is based on a 7×7 sliding window.

Table 5. GLCM features calculated for the extraction of spatial information from Sentinel-2 imagery.

Name	Formula	Description
Entropy	$\sum_{i,j=0}^{n-1} p(i,j) \log(p(i,j))$	Measures the degree of the disorder of neighboring pixels
Correlation	$\frac{\sum_i \sum_j (ij) p(i,j) - \mu_x \mu_y}{\sigma_x \sigma_y}$	Measures the linear dependency of gray levels of neighboring pixels
Contrast	$\sum_{n=0}^{G-1} n^2 \left\{ \sum_{i=1}^G \sum_{j=1}^G P(i,j) \right\}, i-j = n$	Measures the contrast based on the local gray-level distribution
Inverse Difference Moment	$\sum_i \sum_j \frac{1}{1 + (i-j)^2} p(i,j)$	Measures the smoothness (homogeneity) of the gray-level distribution

The second approach is based on an adaptive definition of pixel neighborhoods, i.e., segments, for the extraction of spatial information. A flat zone filter [72] with a minimum object area size of 0.2 ha (5 pixels) was applied to the PC1, generating a segmentation of the image by grouping pixels that share a degree of similarity in their spectral information. For each individual pixel, spatial information was extracted by computing the median in each Sentinel-2 band for pixels that belong in the same segment [73,74].

The third and final approach for the extraction of spatial information is a combination of the two aforementioned methods. Based on the segmentation of the image created in the previous method, spatial information for each pixel is computed as the mean value of all GLCM features of pixels that belong in the same segment.

Two feature vectors are extracted for every point. The first feature vector corresponds to the spectral information that is derived directly from the Sentinel-2 bands, containing 7 features in total (7 spectral bands). The second feature vector contains the spatial information. When examining the use of GLCM features in either of the two approaches, the feature vector contained 4 features. When examining the use of the object median calculations as a means of extracting spatial information, the feature vector contained 7 band features in total. By merging both feature vectors, a multi-source dataset is generated, containing all available optical and contextual spatial information.

RF classifiers were selected as the machine learning algorithms to be used for the classification task. To find the best set of hyperparameters and best performance metrics for the RF models, a nested 5-fold cross-validation with an inner 3-fold cross-validation was conducted. Concerning the model's tuning, the hyperparameter number of trees and maximum depth were investigated. Assessment of the model's performance in the hyperparameter grid search was carried out based on the accuracy metric. After identifying the best set of hyperparameters, the models were trained and applied to each study area to obtain the final tree cover density map. A flowchart highlighting the process for all proposed approaches tested can be found in Figure 2.

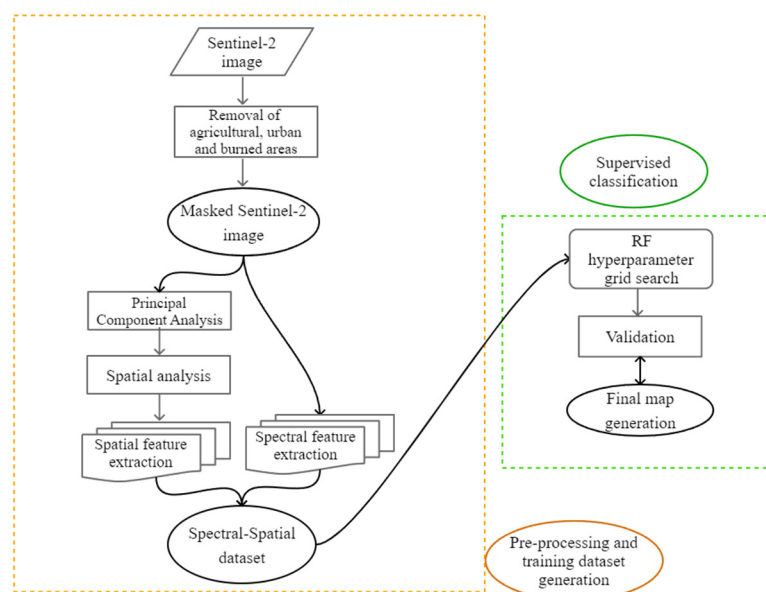


Figure 2. Flowchart of the spectral-spatial workflow for the classification of tree cover density in Mediterranean ecosystems.

2.5. Accuracy Assessment

The identification of tree cover density in areas with a complex vegetation structure is a challenging task, especially when the mapping is performed over large areas where field sampling is not an option. To create the testing set of this research, a series of sampling points was generated randomly over the 3 study areas, only in areas not designated as agricultural or urban. Points located inside burned areas were also excluded. Each point was assigned to one of the 3 target classes via photo-interpretation by experts, utilizing Google Earth high-resolution images. In total, 3309 testing patterns were generated and distributed among the different areas, as seen in Table 6. For the assessment of the performance of the trained models, the Precision, Recall, and F1-score (harmonized mean of the precision and recall metrics) metrics are used [75–77], as some of the most well-

established and frequently used metrics for classification tasks. The assessment also takes into account the average metric scores from all classes and the overall accuracy (OA) of the model. Finally, for each class result, the support metric is also presented, highlighting the number of available testing samples that were present for the extraction of the respective metrics.

Table 6. Validation points generated for the accuracy assessment of each study area.

Study Area	Validation Points
A	810
B	1748
C	751
Total	3309

3. Results

3.1. Study Area A

The results obtained from the validation of the tree cover density maps for the study area A are presented in Table 7 and Figure 3. More specifically, the approach using only Sentinel-2 data performs similarly to the approaches that rely on the GLCM calculations, indicating that spatial information did not consistently improve results across all classes. Overall, the approach that combines the spectral information with the spatial data, as the median values of all connected pixels, outperforms all, achieving an overall accuracy of 85.54%, with individual precision, recall, and F1-score averages being 76.72%, 73.84%, and 75.15%, respectively.

Table 7. Performance results of the tested approaches for the classification of tree cover density for study area A.

Method	Classes	Precision (%)	Recall (%)	F1-Score (%)	Support	OA (%)
Sentinel-2	Non-forest	89.29	86.58	87.92	626	79.36
	Open forest	41.03	52.03	45.88	123	
	Closed forest	78.26	60	67.92	60	
	Average	69.53	66.20	67.24		
Sentinel-2 + GLCM	Non-forest	88.59	83.07	85.74	626	76.39
	Open forest	35.23	50.41	41.47	123	
	Closed forest	78.26	60	67.92	60	
	Average	67.36	64.49	65.04		
Sentinel-2 + GLCM (object-based)	Non-forest	88.58	85.46	86.99	626	78
	Open forest	36.36	45.53	40.43	123	
	Closed forest	78.43	66.67	72.07	60	
	Average	67.79	65.89	66.50		
Sentinel-2 + object statistics (median)	Non-forest	91.44	92.17	91.81	626	85.54
	Open forest	57.94	59.35	58.63	123	
	Closed forest	80.77	70	75	60	
	Average	76.72	73.84	75.15		

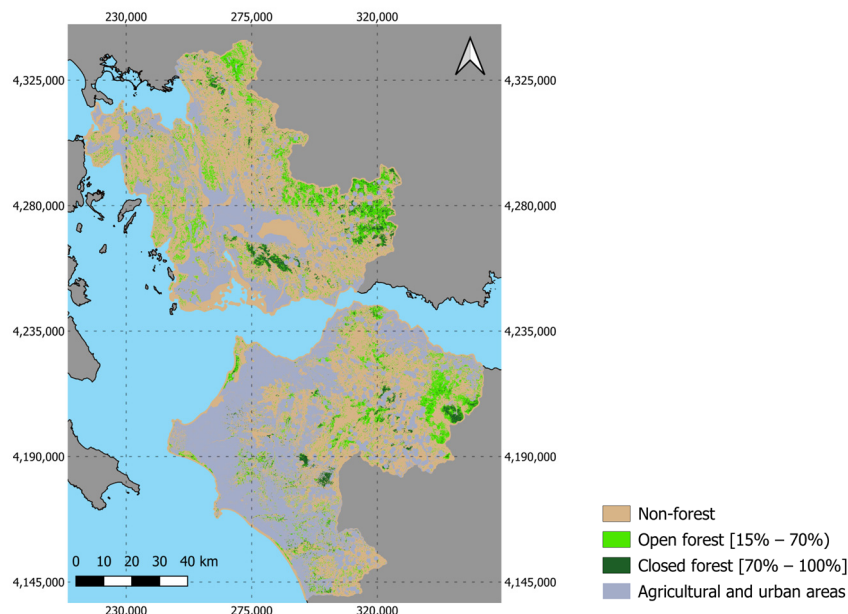


Figure 3. Tree cover density map generated using the best-performing method for study area A in GRS87 coordinate reference system.

3.2. Study Area B

The results obtained from the validation of the tree cover density maps for the study area of B are presented in Table 8 and Figure 4. Similarly to the case of study area A, GLCM textural feature extraction produces similar results to using only spectral data, indicating that the extra information introduced in the classification process does not help improve results. In the case of the approach using GLCM features, a small increase is notable in the correct classification of samples that have been assigned to the open forest class (Recall metric). The approach that combines the spectral with the spatial median data again is highlighted as the best, achieving an overall accuracy of 77.28%, with individual precision, recall, and F1-score averages being 73.75%, 68.95%, and 70.43%, respectively.

Table 8. Performance results of the tested approaches for the classification of tree cover density for study area B.

Method	Classes	Precision (%)	Recall (%)	F1-Score (%)	Support	OA (%)
Sentinel-2	Non-forest	79.65	91.89	85.34	950	73.10
	Open forest	39.55	41.89	40.69	339	
	Closed forest	89.73	57.21	69.87	458	
	Average	69.64	63.66	65.30		
Sentinel-2 + GLCM	Non-forest	82.38	89.05	85.58	950	72.81
	Open forest	39.73	51.33	44.79	339	
	Closed forest	89.36	55.02	68.11	458	
	Average	70.49	65.13	66.16		
Sentinel-2 + GLCM (object-based)	Non-forest	79.57	92.63	85.60	950	73.10
	Open forest	39.61	41.59	40.58	339	
	Closed forest	89.82	55.90	68.91	458	
	Average	69.67	63.37	65.03		
Sentinel-2 + object statistics (median)	Non-forest	83.05	93.89	88.14	950	77.28
	Open forest	47.88	49.85	48.84	339	
	Closed forest	90.31	63.10	74.29	458	
	Average	73.75	68.95	70.43		

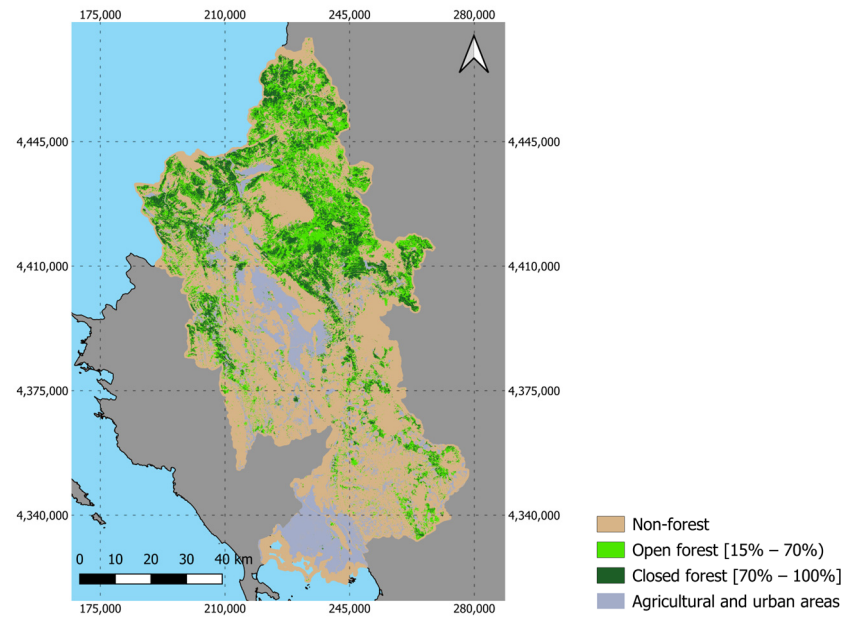


Figure 4. Tree cover density map generated using the best-performing method for study area B in GGRS87 coordinate reference system.

3.3. Study Area C

The results obtained from the validation of the tree cover density maps for the study area of C are presented in Table 9 and Figure 5. In this case, both approaches that rely on the GLCM features perform better than when using only the multispectral Sentinel-2 images. This increase in classification performance is attributed to the non-forest class that is detected better. The approach that combines the spectral with the spatial median data proved to be the best-performing candidate, reaching almost 80% in overall accuracy, while precision, recall, and F1-score class average scores were 75.51%, 73.60%, and 72.22%, respectively.

Table 9. Performance results of the tested approaches for the classification of tree cover density for study area C.

Method	Classes	Precision (%)	Recall (%)	F1-Score (%)	Support	OA (%)
Sentinel-2	Non-forest	51.94	84.28	64.27	159	75.63
	Open forest	64.63	38.41	48.18	138	
	Closed forest	92.70	83.92	88.09	454	
	Average	69.76	68.87	66.85		
Sentinel-2 + GLCM	Non-forest	54.25	84.28	66.01	159	76.43
	Open forest	63.16	34.78	44.86	138	
	Closed forest	91.59	86.34	88.89	454	
	Average	69.67	68.47	66.59		
Sentinel-2 + GLCM (object-based)	Non-forest	53.33	80.50	64.16	159	75.77
	Open forest	62.16	33.33	43.40	138	
	Closed forest	90.39	87.00	88.66	454	
	Average	68.63	66.95	65.41		
Sentinel-2 + object statistics (median)	Non-forest	56.73	87.42	68.81	159	79.63
	Open forest	76.19	46.38	57.66	138	
	Closed forest	93.60	87.00	90.18	454	
	Average	75.51	73.60	72.22		

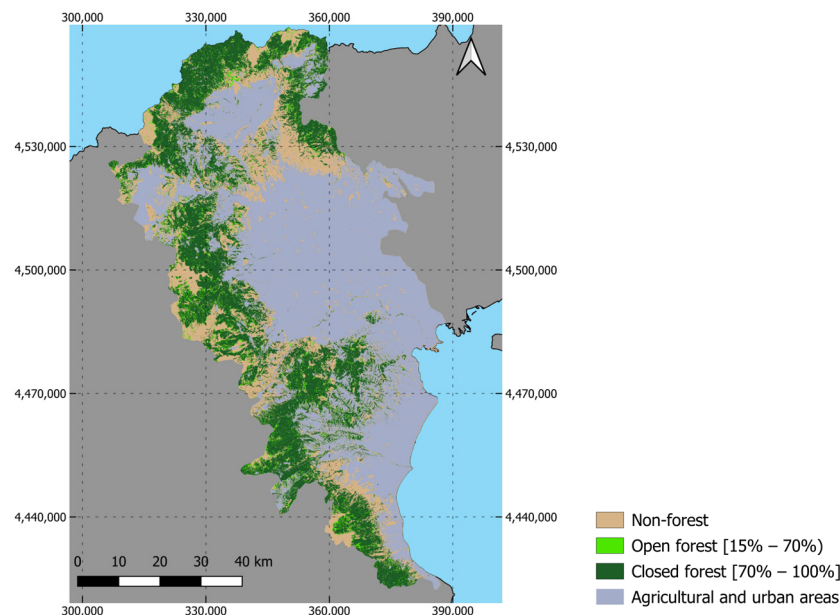


Figure 5. Tree cover density map generated using the best-performing method for study area C in GGRS87 coordinate reference system.

4. Discussion

One of the principal aims of this research is the development of a process that makes use of single-date multispectral imagery and enables the extraction of tree cover density information in large areas. The approach classifies areas in broad density classes, mainly aiming to create exploitable products in the context of fuel mapping. Based on the results that are produced from the validation process, the method proposed allows a promising separation of areas based on their tree cover density and enables the generation of accurate canopy cover maps.

So far, fuel mapping efforts in Greek territories relied on static outdated products as a means of integrating tree cover density information [66,67]. The method proposed in this research enables the timely generation of updatable tree cover density information layers, providing an alternative that can be utilized in future fuel mapping works. A single summer cloud-free Sentinel-2 image is utilized from the summer months, allowing the approach to capture a snapshot of different dynamic processes at a time when the leaf area reaches its peak. Yang et al. [78] demonstrated that fractional vegetation cover (FVC) and Leaf Area Index (LAI), which are directly correlated with tree cover density, reached their maximum values in August, leading to maximum overall forest canopy (OFC). Therefore, late summer images provide the best representation for the classification of forest canopy cover. The single image approach was opted over a potential multi-temporal image analysis, which would not contribute to a more accurate classification since it would consider spectral vegetation characteristics from seasons without or with less tree cover, potentially resulting in more errors and underestimation of actual tree cover.

The results presented in Tables 7–9 lead to the conclusion that out of the three target classes, only one cannot be very well identified, i.e., the open forest class. On the other hand, the non-forest and the closed forest classes display good detection results (F1-scores > 60% in all cases). This can be potentially attributed to the fact that when the tree canopy is sparse, it allows more information from the understory to be captured by the multispectral sensors. Shrubs, grasses, and non-vegetated areas located beneath the canopy will produce a mixed spectral signature, introducing more noise in the system and hindering the performance of the classifiers. Similar results have been verified in other studies that addressed the topic of tree cover density estimation [69,79,80]. More specifically, the results produced by the research of Nasiri et al. [80], demonstrate that sparse and medium-density Mediterranean forests (which account roughly for the open class in this study) can produce F1-scores that

are more than 20% lower, when compared with the dense cover and non-forest counterparts. A similar conclusion is also reached by [79], whose open class (defined with a cover of 10%–40%) also exhibits the lowest results when compared with other densities.

The incorporation of GLCM features, as a means of identifying underlying spatial patterns between pixels, provided inconclusive results in the types of Mediterranean ecosystems examined. Performance metrics were improved in certain classes, e.g., the closed forest class in West Greece. However, no clear results are reached in terms of large-scale mapping of canopy cover between the three of them. The findings produced in this research are aligned with many other studies that have reached similar conclusions. Huang et al. [48], after an extensive investigation of tree cover density estimation capacity from very high-resolution and medium-resolution sensors, concluded that texture information derived from GLCM is beneficial at higher spatial resolutions (<5 m) but no longer plays a significant role when using medium-resolution images. Godinho et al. [81] also report that spectral information is considered more important than GLCM features in Landsat 8 images.

In our work, we considered the guidelines of Hall-Beyer for the definition of the GLCM features [71]. More specifically, a lot of the GLCM features are correlated with each other, as some describe edge-like characteristics, while others are better at expressing characteristics of the interior. In the end, only a few of them are required, and they can be selected beforehand by the researchers empirically, while at the same time ensuring that performance is not significantly affected. Furthermore, again based on Hall-Beyer, window sizes do not exhibit significant changes in the textural information that is captured in most cases. As a result, the author concludes that in the case of using GLCM features, researchers can, in most cases, define the initial features and use them without performing an exhaustive search of all factors that may define the GLCM method, which may be outside the scope of the research conducted. Overall, there are numerous different GLCM features that can be calculated and windows or parameters that can be used. In the scope of this work, the GLCM analysis was defined initially as advised in [71] and was not investigated extensively. Based on the results that are reached in this investigation, there is room for potential future research that may investigate specific aspects of GLCM textures and how tree cover density mapping can be improved in complex Mediterranean ecosystems.

Regarding the non-GLCM spatial information extraction method that is proposed, i.e., the extraction of spatial information as the median of the spectral values of all connected pixels, promising results were achieved. Using this best approach, the overall classification accuracy achieved in all of the three areas ranged from 77% to 85%. F1-scores were also similarly high, ranging from 70% to 75%, which is a substantial increase in terms of performance gain when compared to the other tested alternatives. As reported in [48], spectral information in medium resolutions plays a decisive role in the mapping of tree cover density. Our approach manages to successfully build upon that by integrating spatial information as a descriptive statistic of spectral values of larger regions, defining a viable way to enhance tree cover density products. To the authors' knowledge, no similar approach has been used in previous works in the context of mapping tree cover densities, effectively highlighting a viable and robust approach that can be expanded in future research.

Finally, one of the objectives of this research was to present a viable method for the mapping of tree density in Mediterranean ecosystems. Given the large area covered by this study, photo-interpretation of very high-resolution imagery was selected as the best means of producing the training and validation datasets following a number of studies that used similar practices [27,31,41,48]. Despite small variations in the distributions of the training and validation points in each study area, the results produced are consistent, irrespective of the different density classes' distributions, landscapes, and vegetation zones, supporting the validity of the proposed workflow.

Although this study accomplished its objectives, some limitations need to be mentioned. More specifically, the research examined only the RF classifier as one of the most widely used algorithms in this kind of application. Future research could expand further

by addressing a more holistic investigation of different classification algorithms in terms of their ability to map tree cover density. Regarding the GLCM calculations, our approach did not take into consideration an exhaustive investigation of all features and potential methods of calculations but instead followed well-established guidelines for the selection of GLCM textures. Finally, the study focuses specifically on the three broad forest cover density classes, as defined by the fuel mapping requirements established by the FirEUrisk project. As a result, while the methodology provides promising results that can be transferred to other similar biomes, it is mainly to be used within the scope of fuel mapping as other potential applications may require a more detailed separation of density.

5. Conclusions

This study aimed at the development of a spectral–spatial classification approach that would enable the accurate and updatable mapping of tree canopy cover in Greek territories from single-date Sentinel-2 multispectral images. Three methods are examined in terms of their capacity to enhance the mapping of the different tree cover densities required. Results indicate that tree cover can be estimated with promising accuracy in Mediterranean landscapes characterized by a complex structure and rough topography. More specifically:

- The introduction of GLCM textural features in the classification process as a means of extracting spatial information, overall, did not yield any consistent results, allowing better identification of certain tree cover density classes only.
- Similarly, the aggregation of GLCM information inside object boundaries did help enhance classification performance.
- The extraction of spatial information, as the median of Sentinel-2 spectral values for pixels that belong in the same segment, provided the most accurate results and consistently improved performance when compared to the other alternatives.

Overall, it is well established that Sentinel-2 images can successfully contribute to the mapping of tree cover density in Mediterranean biomes. This study aids in improving the identification of tree cover through the development of a robust and accurate approach that allows the generation of updatable tree cover density maps. These maps can be integrated into fuel mapping products, providing an additional layer of information and subsequently providing enhanced support to wildfire prevention actions and informed decision-making. Given certain limitations of the study, it would be interesting to perform a more extensive investigation of machine learning classification algorithms and GLCM features for the mapping of tree cover density in Mediterranean ecosystems, potentially also exploiting information derived from Sentinel-1. Further research could also focus on the use of the proposed approach to a national extent, performing a more holistic mapping of tree cover in Greek territories and, at the same time, assessing its capabilities and computational challenges in an operational capacity.

Author Contributions: Conceptualization, M.S., I.Z.G. and D.S.; methodology, M.S. and N.G.; software, M.S.; validation, M.S., K.A. and E.G.; formal analysis, M.S.; investigation, M.S.; resources, M.S.; data curation, M.S., K.A. and E.G.; writing—original draft preparation, M.S.; writing—review and editing, M.S., I.Z.G. and N.G.; visualization, M.S.; supervision, I.Z.G. and D.S.; project administration, I.Z.G.; funding acquisition, M.S. and I.Z.G. All authors have read and agreed to the published version of the manuscript.

Funding: This research was financed by the project FirEUrisk—Developing a Holistic, Risk-Wise Strategy for European Wildfire Management, funded by the European Union’s Horizon 2020 research and innovation programme under grant agreement No. 101003890. This research was also supported by the Special Account for Research Funds of the Aristotle University of Thessaloniki through the Action “Excellence Scholarships For PhD Candidates Of The Faculties: Engineering, Sciences, Agriculture, Forestry and Natural Environment”.

Data Availability Statement: The raw data supporting the conclusions of this article could be made available by the authors on request.

Conflicts of Interest: The authors declare no conflicts of interest.

References

- Dong, J.; Kaufmann, R.K.; Myneni, R.B.; Tucker, C.J.; Kauppi, P.E.; Liski, J.; Buermann, W.; Alexeyev, V.; Hughes, M.K. Remote Sensing Estimates of Boreal and Temperate Forest Woody Biomass: Carbon Pools, Sources, and Sinks. *Remote Sens. Environ.* **2003**, *84*, 393–410. [\[CrossRef\]](#)
- Foody, G.M. Status of Land Cover Classification Accuracy Assessment. *Remote Sens. Environ.* **2002**, *80*, 185–201. [\[CrossRef\]](#)
- Wulder, M.A.; Franklin, S.E. (Eds.) Understanding Forest Disturbance and Spatial Pattern. In *Remote Sensing and GIS Approaches*; CRC Press: Boca Raton, FL, USA, 2006; ISBN 978-0-429-11443-4.
- Gschwantner, T.; Schadauer, K.; Vidal, C.; Lanz, A.; Tomppo, E.; Di Cosmo, L.; Robert, N.; Englert Duursma, D.; Lawrence, M. Common Tree Definitions for National Forest Inventories in Europe. *Silva Fenn.* **2009**, *43*, 463. [\[CrossRef\]](#)
- Sadeghi, S.M.M.; Gordon, D.A.; Van Stan, J.T., II. A Global Synthesis of Throughfall and Stemflow Hydrometeorology. In *Precipitation Partitioning by Vegetation*; Van Stan, J.T., II, Gutmann, E., Friesen, J., Eds.; Springer International Publishing: Cham, Switzerland, 2020; pp. 49–70, ISBN 978-3-030-29701-5.
- Xu, H.; Hu, X.; Guan, H.; Zhang, B.; Wang, M.; Chen, S.; Chen, M. A Remote Sensing Based Method to Detect Soil Erosion in Forests. *Remote Sens.* **2019**, *11*, 513. [\[CrossRef\]](#)
- Li, S.; Hou, Z.; Ge, J.; Wang, T. Assessing the Effects of Large Herbivores on the Three-Dimensional Structure of Temperate Forests Using Terrestrial Laser Scanning. *For. Ecol. Manag.* **2022**, *507*, 119985. [\[CrossRef\]](#)
- Awasthi, N.; Aryal, K.; Bahadur Khanal Chhetri, B.; Bhandari, S.K.; Khanal, Y.; Gotame, P.; Baral, K. Reflecting on Species Diversity and Regeneration Dynamics of Scientific Forest Management Practices in Nepal. *For. Ecol. Manag.* **2020**, *474*, 118378. [\[CrossRef\]](#)
- Korhonen, L.; Korhonen, K.; Rautiainen, M.; Stenberg, P. Estimation of Forest Canopy Cover: A Comparison of Field Measurement Techniques. *Silva Fenn.* **2006**, *40*, 315. [\[CrossRef\]](#)
- Song, C.; Schroeder, T.; Cohen, W. Predicting Temperate Conifer Forest Successional Stage Distributions with Multitemporal Landsat Thematic Mapper Imagery. *Remote Sens. Environ.* **2007**, *106*, 228–237. [\[CrossRef\]](#)
- Hansen, M.C.; DeFries, R.S.; Townshend, J.R.G.; Carroll, M.; Dimiceli, C.; Sohlberg, R.A. Global Percent Tree Cover at a Spatial Resolution of 500 Meters: First Results of the MODIS Vegetation Continuous Fields Algorithm. *Earth Interact.* **2003**, *7*, 1–15. [\[CrossRef\]](#)
- Sexton, J.O.; Song, X.-P.; Feng, M.; Noojipady, P.; Anand, A.; Huang, C.; Kim, D.-H.; Collins, K.M.; Channan, S.; DiMiceli, C.; et al. Global, 30-m Resolution Continuous Fields of Tree Cover: Landsat-Based Rescaling of MODIS Vegetation Continuous Fields with Lidar-Based Estimates of Error. *Int. J. Digit. Earth* **2013**, *6*, 427–448. [\[CrossRef\]](#)
- Cohen, W.B.; Goward, S.N. Landsat's Role in Ecological Applications of Remote Sensing. *Bioscience* **2004**, *54*, 535. [\[CrossRef\]](#)
- Wulder, M.A.; White, J.C.; Goward, S.N.; Masek, J.G.; Irons, J.R.; Herold, M.; Cohen, W.B.; Loveland, T.R.; Woodcock, C.E. Landsat Continuity: Issues and Opportunities for Land Cover Monitoring. *Remote Sens. Environ.* **2008**, *112*, 955–969. [\[CrossRef\]](#)
- Yang, J.; Weisberg, P.J.; Bristow, N.A. Landsat Remote Sensing Approaches for Monitoring Long-Term Tree Cover Dynamics in Semi-Arid Woodlands: Comparison of Vegetation Indices and Spectral Mixture Analysis. *Remote Sens. Environ.* **2012**, *119*, 62–71. [\[CrossRef\]](#)
- Carreiras, J.M.B.; Pereira, J.M.C.; Pereira, J.S. Estimation of Tree Canopy Cover in Evergreen Oak Woodlands Using Remote Sensing. *For. Ecol. Manag.* **2006**, *223*, 45–53. [\[CrossRef\]](#)
- Donmez, C.; Berberoglu, S.; Erdogan, M.A.; Tanriover, A.A.; Cilek, A. Response of the Regression Tree Model to High Resolution Remote Sensing Data for Predicting Percent Tree Cover in a Mediterranean Ecosystem. *Environ. Monit. Assess.* **2015**, *187*, 4. [\[CrossRef\]](#)
- Griffiths, P.; Kuemmerle, T.; Baumann, M.; Radeloff, V.C.; Abrudan, I.V.; Lieskovsky, J.; Munteanu, C.; Ostapowicz, K.; Hostert, P. Forest Disturbances, Forest Recovery, and Changes in Forest Types across the Carpathian Ecoregion from 1985 to 2010 Based on Landsat Image Composites. *Remote Sens. Environ.* **2014**, *151*, 72–88. [\[CrossRef\]](#)
- Halperin, J.; LeMay, V.; Coops, N.; Verchot, L.; Marshall, P.; Lochhead, K. Canopy Cover Estimation in Miombo Woodlands of Zambia: Comparison of Landsat 8 OLI versus RapidEye Imagery Using Parametric, Nonparametric, and Semiparametric Methods. *Remote Sens. Environ.* **2016**, *179*, 170–182. [\[CrossRef\]](#)
- Kobayashi, T.; Tsend-Ayush, J.; Tateishi, R. A New Global Tree-Cover Percentage Map Using MODIS Data. *Int. J. Remote Sens.* **2016**, *37*, 969–992. [\[CrossRef\]](#)
- Korhonen, L.; Ali-Sisto, D.; Tokola, T. Tropical Forest Canopy Cover Estimation Using Satellite Imagery and Airborne Lidar Reference Data. *Silva Fenn.* **2015**, *49*, 1405. [\[CrossRef\]](#)
- Cilek, A.; Berberoglu, S.; Donmez, C.; Sahingoz, M. The Use of Regression Tree Method for Sentinel-2 Satellite Data to Mapping Percent Tree Cover in Different Forest Types. *Environ. Sci. Pollut. Res.* **2022**, *29*, 23665–23676. [\[CrossRef\]](#)
- Korhonen, L.; Hadi; Packalen, P.; Rautiainen, M. Comparison of Sentinel-2 and Landsat 8 in the Estimation of Boreal Forest Canopy Cover and Leaf Area Index. *Remote Sens. Environ.* **2017**, *195*, 259–274. [\[CrossRef\]](#)
- Anchang, J.Y.; Prihodko, L.; Ji, W.; Kumar, S.S.; Ross, C.W.; Yu, Q.; Lind, B.; Sarr, M.A.; Diouf, A.A.; Hanan, N.P. Toward Operational Mapping of Woody Canopy Cover in Tropical Savannas Using Google Earth Engine. *Front. Environ. Sci.* **2020**, *8*, 4. [\[CrossRef\]](#)

25. Zhang, W.; Brandt, M.; Wang, Q.; Prishchepov, A.V.; Tucker, C.J.; Li, Y.; Lyu, H.; Fensholt, R. From Woody Cover to Woody Canopies: How Sentinel-1 and Sentinel-2 Data Advance the Mapping of Woody Plants in Savannas. *Remote Sens. Environ.* **2019**, *234*, 111465. [[CrossRef](#)]
26. Astola, H.; Häme, T.; Sirro, L.; Molinier, M.; Kilpi, J. Comparison of Sentinel-2 and Landsat 8 Imagery for Forest Variable Prediction in Boreal Region. *Remote Sens. Environ.* **2019**, *223*, 257–273. [[CrossRef](#)]
27. Bera, D.; Das Chatterjee, N.; Bera, S.; Ghosh, S.; Dinda, S. Comparative Performance of Sentinel-2 MSI and Landsat-8 OLI Data in Canopy Cover Prediction Using Random Forest Model: Comparing Model Performance and Tuning Parameters. *Adv. Space Res.* **2023**, *71*, 4691–4709. [[CrossRef](#)]
28. Lucas, R.M.; Clewley, D.; Accad, A.; Butler, D.; Armston, J.; Bowen, M.; Bunting, P.; Carreiras, J.; Dwyer, J.; Eyre, T.; et al. Mapping Forest Growth and Degradation Stage in the Brigalow Belt Bioregion of Australia through Integration of ALOS PALSAR and Landsat-Derived Foliage Projective Cover Data. *Remote Sens. Environ.* **2014**, *155*, 42–57. [[CrossRef](#)]
29. Smith, A.M.S.; Falkowski, M.J.; Hudak, A.T.; Evans, J.S.; Robinson, A.P.; Steele, C.M. A Cross-Comparison of Field, Spectral, and Lidar Estimates of Forest Canopy Cover. *Can. J. Remote Sens.* **2009**, *35*, 447–459. [[CrossRef](#)]
30. Alexander, C.; Bøcher, P.K.; Arge, L.; Svenning, J.-C. Regional-Scale Mapping of Tree Cover, Height and Main Phenological Tree Types Using Airborne Laser Scanning Data. *Remote Sens. Environ.* **2014**, *147*, 156–172. [[CrossRef](#)]
31. Adjognon, G.S.; Rivera-Ballesteros, A.; Van Soest, D. Satellite-Based Tree Cover Mapping for Forest Conservation in the Drylands of Sub Saharan Africa (SSA): Application to Burkina Faso Gazetted Forests. *Dev. Eng.* **2019**, *4*, 100039. [[CrossRef](#)]
32. Breiman, L. Random Forests. *Mach. Learn.* **2001**, *45*, 5–32. [[CrossRef](#)]
33. Duro, D.C.; Franklin, S.E.; Dubé, M.G. A Comparison of Pixel-Based and Object-Based Image Analysis with Selected Machine Learning Algorithms for the Classification of Agricultural Landscapes Using SPOT-5 HRG Imagery. *Remote Sens. Environ.* **2012**, *118*, 259–272. [[CrossRef](#)]
34. Gislason, P.O.; Benediktsson, J.A.; Sveinsson, J.R. Random Forests for Land Cover Classification. *Pattern Recognit. Lett.* **2006**, *27*, 294–300. [[CrossRef](#)]
35. Rodriguez-Galiano, V.F.; Chica-Olmo, M.; Abarca-Hernandez, F.; Atkinson, P.M.; Jeganathan, C. Random Forest Classification of Mediterranean Land Cover Using Multi-Seasonal Imagery and Multi-Seasonal Texture. *Remote Sens. Environ.* **2012**, *121*, 93–107. [[CrossRef](#)]
36. Chan, J.C.-W.; Paelinckx, D. Evaluation of Random Forest and Adaboost Tree-Based Ensemble Classification and Spectral Band Selection for Ecotope Mapping Using Airborne Hyperspectral Imagery. *Remote Sens. Environ.* **2008**, *112*, 2999–3011. [[CrossRef](#)]
37. Son, N.-T.; Chen, C.-F.; Chen, C.-R.; Minh, V.-Q. Assessment of Sentinel-1A Data for Rice Crop Classification Using Random Forests and Support Vector Machines. *Geocarto Int.* **2017**, *33*, 587–601. [[CrossRef](#)]
38. Belgiu, M.; Drăguț, L. Random Forest in Remote Sensing: A Review of Applications and Future Directions. *ISPRS J. Photogramm. Remote Sens.* **2016**, *114*, 24–31. [[CrossRef](#)]
39. Baccini, A.; Laporte, N.; Goetz, S.J.; Sun, M.; Dong, H. A First Map of Tropical Africa’s above-Ground Biomass Derived from Satellite Imagery. *Environ. Res. Lett.* **2008**, *3*, 045011. [[CrossRef](#)]
40. Eisavi, V.; Homayouni, S.; Yazdi, A.M.; Alimohammadi, A. Land Cover Mapping Based on Random Forest Classification of Multitemporal Spectral and Thermal Images. *Environ. Monit. Assess.* **2015**, *187*, 291. [[CrossRef](#)]
41. Freeman, E.A.; Moisen, G.G.; Coulston, J.W.; Wilson, B.T. Random Forests and Stochastic Gradient Boosting for Predicting Tree Canopy Cover: Comparing Tuning Processes and Model Performance. *Can. J. For. Res.* **2016**, *46*, 323–339. [[CrossRef](#)]
42. Coulston, J.W.; Moisen, G.G.; Wilson, B.T.; Finco, M.V.; Cohen, W.B.; Brewer, C.K. Modeling Percent Tree Canopy Cover: A Pilot Study. *Photogramm. Eng. Remote Sens.* **2012**, *78*, 715–727. [[CrossRef](#)]
43. Goldblatt, R.; Rivera Ballesteros, A.; Burney, J. High Spatial Resolution Visual Band Imagery Outperforms Medium Resolution Spectral Imagery for Ecosystem Assessment in the Semi-Arid Brazilian Sertão. *Remote Sens.* **2017**, *9*, 1336. [[CrossRef](#)]
44. Puletti, N.; Chianucci, F.; Castaldi, C. Use of Sentinel-2 for Forest Classification in Mediterranean Environments. *Ann Silv. Res* **2018**, *42*, 32–38.
45. Powell, S.L.; Cohen, W.B.; Healey, S.P.; Kennedy, R.E.; Moisen, G.G.; Pierce, K.B.; Ohmann, J.L. Quantification of Live Aboveground Forest Biomass Dynamics with Landsat Time-Series and Field Inventory Data: A Comparison of Empirical Modeling Approaches. *Remote Sens. Environ.* **2010**, *114*, 1053–1068. [[CrossRef](#)]
46. Haralick, R.M.; Shanmugam, K.; Dinstein, I. Textural Features for Image Classification. *IEEE Trans. Syst. Man Cybern.* **1973**, *SMC-3*, 610–621. [[CrossRef](#)]
47. Kayitakire, F.; Hamel, C.; Defourny, P. Retrieving Forest Structure Variables Based on Image Texture Analysis and IKONOS-2 Imagery. *Remote Sens. Environ.* **2006**, *102*, 390–401. [[CrossRef](#)]
48. Huang, H.; Wang, Z.; Chen, J.; Shi, Y. Improving Tree Cover Estimation for Sparse Trees Mixed with Herbaceous Vegetation in Drylands Using Texture Features of High-Resolution Imagery. *Forests* **2024**, *15*, 847. [[CrossRef](#)]
49. Karlson, M.; Ostwald, M.; Reese, H.; Sanou, J.; Tankoano, B.; Mattsson, E. Mapping Tree Canopy Cover and Aboveground Biomass in Sudano-Sahelian Woodlands Using Landsat 8 and Random Forest. *Remote Sens.* **2015**, *7*, 10017–10041. [[CrossRef](#)]
50. Guirado, E.; Alcaraz-Segura, D.; Cabello, J.; Puertas-Ruiz, S.; Herrera, F.; Tabik, S. Tree Cover Estimation in Global Drylands from Space Using Deep Learning. *Remote Sens.* **2020**, *12*, 343. [[CrossRef](#)]
51. Zhang, T.; Liu, D. Estimating Fractional Vegetation Cover from Multispectral Unmixing Modeled with Local Endmember Variability and Spatial Contextual Information. *ISPRS J. Photogramm. Remote Sens.* **2024**, *209*, 481–499. [[CrossRef](#)]

52. Hansen, M.C.; Potapov, P.V.; Moore, R.; Hancher, M.; Turubanova, S.A.; Tyukavina, A.; Thau, D.; Stehman, S.V.; Goetz, S.J.; Loveland, T.R.; et al. High-Resolution Global Maps of 21st-Century Forest Cover Change. *Science* **2013**, *342*, 850–853. [[CrossRef](#)]
53. Mora, B.; Tsendbazar, N.-E.; Herold, M.; Arino, O. Global Land Cover Mapping: Current Status and Future Trends. In *Land Use and Land Cover Mapping in Europe*; Manakos, I., Braun, M., Eds.; Remote Sensing and Digital Image Processing; Springer: Dordrecht, The Netherlands, 2014; Volume 18, pp. 11–30. ISBN 978-94-007-7968-6.
54. Asner, G.P. Automated Mapping of Tropical Deforestation and Forest Degradation: CLASlite. *J. Appl. Remote Sens.* **2009**, *3*, 033543. [[CrossRef](#)]
55. Lehmann, E.A.; Wallace, J.F.; Caccetta, P.A.; Furby, S.L.; Zdunic, K. Forest Cover Trends from Time Series Landsat Data for the Australian Continent. *Int. J. Appl. Earth Obs. Geoinf.* **2013**, *21*, 453–462. [[CrossRef](#)]
56. Fisher, A.; Day, M.; Gill, T.; Roff, A.; Danaher, T.; Flood, N. Large-Area, High-Resolution Tree Cover Mapping with Multi-Temporal SPOT5 Imagery, New South Wales, Australia. *Remote Sens.* **2016**, *8*, 515. [[CrossRef](#)]
57. Kennedy, R.E.; Yang, Z.; Cohen, W.B. Detecting Trends in Forest Disturbance and Recovery Using Yearly Landsat Time Series: 1. LandTrendr—Temporal Segmentation Algorithms. *Remote Sens. Environ.* **2010**, *114*, 2897–2910. [[CrossRef](#)]
58. DiMiceli, C.M.; Carroll, M.L.; Sohlberg, R.A.; Huang, C.; Hansen, M.C.; Townshend, J.R. *Annual Global Automated MODIS Vegetation Continuous Fields (MOD44B) at 250 m Spatial Resolution for Data Years Beginning Day 65, 2000–2010, Collection 5 Percent Tree Cover*; University of Maryland: College Park, MD, USA, 2011.
59. McRoberts, R.E.; Cohen, W.B.; Næsset, E.; Stehman, S.V.; Tomppo, E.O. Using Remotely Sensed Data to Construct and Assess Forest Attribute Maps and Related Spatial Products. *Scand. J. For. Res.* **2010**, *25*, 340–367. [[CrossRef](#)]
60. Chen, G.; Hay, G.J.; St-Onge, B. A GEOBIA Framework to Estimate Forest Parameters from Lidar Transects, Quickbird Imagery and Machine Learning: A Case Study in Quebec, Canada. *Int. J. Appl. Earth Obs. Geoinf.* **2012**, *15*, 28–37. [[CrossRef](#)]
61. Stojanova, D.; Panov, P.; Gjorgjioski, V.; Kobler, A.; Džeroski, S. Estimating Vegetation Height and Canopy Cover from Remotely Sensed Data with Machine Learning. *Ecol. Inform.* **2010**, *5*, 256–266. [[CrossRef](#)]
62. Hilker, T.; Wulder, M.A.; Coops, N.C. Update of Forest Inventory Data with Lidar and High Spatial Resolution Satellite Imagery. *Can. J. Remote Sens.* **2008**, *34*, 5–12. [[CrossRef](#)]
63. Aragonese, E.; García, M.; Salis, M.; Ribeiro, L.M.; Chuvieco, E. Classification and Mapping of European Fuels Using a Hierarchical, Multipurpose Fuel Classification System. *Earth Syst. Sci. Data* **2023**, *15*, 1287–1315. [[CrossRef](#)]
64. Brandt, J.; Ertel, J.; Spore, J.; Stolle, F. Wall-to-Wall Mapping of Tree Extent in the Tropics with Sentinel-1 and Sentinel-2. *Remote Sens. Environ.* **2023**, *292*, 113574. [[CrossRef](#)]
65. Moreira, F.; Viedma, O.; Arianoutsou, M.; Curt, T.; Koutsias, N.; Rigolot, E.; Barbati, A.; Corona, P.; Vaz, P.; Xanthopoulos, G.; et al. Landscape—Wildfire Interactions in Southern Europe: Implications for Landscape Management. *J. Environ. Manag.* **2011**, *92*, 2389–2402. [[CrossRef](#)] [[PubMed](#)]
66. Sismanis, M.; Stefanidou, A.; Stavrakoudis, D.; Gitas, I.Z. Wildland Fuel Type Mapping in Attica Using Sentinel-2 Time-Series. In Proceedings of the 2023 8th International Conference on Smart and Sustainable Technologies (SpliTech), Split/Bol, Croatia, 20–23 June 2023; IEEE: Piscataway, NJ, USA, 2023; pp. 1–5.
67. Stefanidou, A.; Gitas, I.Z.; Katagis, T. A National Fuel Type Mapping Method Improvement Using Sentinel-2 Satellite Data. *Geocarto Int.* **2022**, *37*, 1022–1042. [[CrossRef](#)]
68. Mutanga, O.; Masenyama, A.; Sibanda, M. Spectral Saturation in the Remote Sensing of High-Density Vegetation Traits: A Systematic Review of Progress, Challenges, and Prospects. *ISPRS J. Photogramm. Remote Sens.* **2023**, *198*, 297–309. [[CrossRef](#)]
69. Li, Z.; Ota, T.; Mizoue, N. Monitoring Tropical Forest Change Using Tree Canopy Cover Time Series Obtained from Sentinel-1 and Sentinel-2 Data. *Int. J. Digit. Earth* **2024**, *17*, 2312222. [[CrossRef](#)]
70. Tompoulidou, M.; Stefanidou, A.; Grigoriadis, D.; Dragozi, E.; Stavrakoudis, D.; Gitas, I.Z. The Greek National Observatory of Forest Fires (NOFFi). In Proceedings of the RSCy2016 Fourth International Conference on Remote Sensing and Geoinformation of Environment, Paphos, Cyprus, 4–8 April 2016; Themistocleous, K., Hadjimitsis, D.G., Michaelides, S., Papadavid, G., Eds.; SPIE: Bellingham, WA, USA, 2016; p. 96880N.
71. Hall-Beyer, M. Practical Guidelines for Choosing GLCM Textures to Use in Landscape Classification Tasks over a Range of Moderate Spatial Scales. *Int. J. Remote Sens.* **2017**, *38*, 1312–1338. [[CrossRef](#)]
72. Salembier, P.; Serra, J. Flat Zones Filtering, Connected Operators, and Filters by Reconstruction. *IEEE Trans. Image Process.* **1995**, *4*, 1153–1160. [[CrossRef](#)]
73. Benediktsson, J.A.; Palmason, J.A.; Sveinsson, J.R. Classification of Hyperspectral Data from Urban Areas Based on Extended Morphological Profiles. *IEEE Trans. Geosci. Remote Sens.* **2005**, *43*, 480–491. [[CrossRef](#)]
74. Fauvel, M.; Chanussot, J.; Benediktsson, J.A. A Spatial–Spectral Kernel-Based Approach for the Classification of Remote-Sensing Images. *Pattern Recognit.* **2012**, *45*, 381–392. [[CrossRef](#)]
75. Goutte, C.; Gaussier, E. A Probabilistic Interpretation of Precision, Recall and F-Score, with Implication for Evaluation. In *Advances in Information Retrieval*; Losada, D.E., Fernández-Luna, J.M., Eds.; Lecture Notes in Computer Science; Springer: Heidelberg/Berlin, Germany, 2005; Volume 3408, pp. 345–359. ISBN 978-3-540-25295-5.
76. Manning, C.D.; Raghavan, P.; Schütze, H. *Introduction to Information Retrieval*, 1st ed.; Cambridge University Press: Cambridge, UK, 2008; ISBN 978-0-521-86571-5.
77. Sokolova, M.; Lapalme, G. A Systematic Analysis of Performance Measures for Classification Tasks. *Inf. Process. Manag.* **2009**, *45*, 427–437. [[CrossRef](#)]

78. Yang, G.; Pu, R.; Zhang, J.; Zhao, C.; Feng, H.; Wang, J. Remote Sensing of Seasonal Variability of Fractional Vegetation Cover and Its Object-Based Spatial Pattern Analysis over Mountain Areas. *ISPRS J. Photogramm. Remote Sens.* **2013**, *77*, 79–93. [[CrossRef](#)]
79. Verhegghen, A.; Kuzelova, K.; Syrris, V.; Eva, H.; Achard, F. Mapping Canopy Cover in African Dry Forests from the Combined Use of Sentinel-1 and Sentinel-2 Data: Application to Tanzania for the Year 2018. *Remote Sens.* **2022**, *14*, 1522. [[CrossRef](#)]
80. Nasiri, V.; Sadeghi, S.M.M.; Moradi, F.; Afshari, S.; Deljouei, A.; Griess, V.C.; Maftei, C.; Borz, S.A. The Influence of Data Density and Integration on Forest Canopy Cover Mapping Using Sentinel-1 and Sentinel-2 Time Series in Mediterranean Oak Forests. *ISPRS Int. J. Geo-Inf.* **2022**, *11*, 423. [[CrossRef](#)]
81. Godinho, S.; Guiomar, N.; Gil, A. Estimating Tree Canopy Cover Percentage in a Mediterranean Silvopastoral Systems Using Sentinel-2A Imagery and the Stochastic Gradient Boosting Algorithm. *Int. J. Remote Sens.* **2018**, *39*, 4640–4662. [[CrossRef](#)]

Disclaimer/Publisher’s Note: The statements, opinions and data contained in all publications are solely those of the individual author(s) and contributor(s) and not of MDPI and/or the editor(s). MDPI and/or the editor(s) disclaim responsibility for any injury to people or property resulting from any ideas, methods, instructions or products referred to in the content.